Proceedings of the 19th International Symposium on the
Packaging and Transportation of Radioactive Materials
PATRAM 2019
August 4-9, 2019, New Orleans, LA, USA

INVESTIGATING THE DEPENDENCE OF HYDROGEN AND OXYGEN GENERATION FROM HIGH-PURITY PLUTONIUM OXIDES IN SEALED CONTAINERS

D. Kirk Veirs   **Mary Ann Stroud**   **Joshua E. Narlesky**   **John M. Berg**

Edward L. Romero   **Daniel Rios**   **Kennard V. Wilson**   **Laura A. Worl**

Los Alamos National Laboratory, P.O. Box 1663, Los Alamos, NM 87545

ABSRACT

Gas generation experiments are being conducted on moist high-purity plutonium oxides in sealed containers to study pressure changes over time. Hydrogen and oxygen are of particular interest because of their potential to form flammable mixtures in containers during transport or storage. A broad range of high-purity plutonium oxides was chosen to investigate dependencies of the maximum hydrogen pressure and $G(H_2)$ (molecules of hydrogen per 100 eV) on the radiation dose to the water, the specific surface area and the number of monolayers (ML) of water adsorbed on the plutonium oxide surface. The specific activity (SA) of the materials ranges from 2.1 to 14.7 W kg^{-1}, and the specific surface area (SSA) ranges from 0.8 to 21.5 m^2 g^{-1}. Flammable mixtures of hydrogen and oxygen that persisted for months were observed in some containers. A set of kinetic models that assumed first order formation and consumption reactions were used to fit the partial pressures of hydrogen and oxygen to obtain the initial rates of production and the maximum partial pressures in the container. Initial rates of hydrogen formation and maximum partial pressures increase with the amount of adsorbed water for materials with the same SSA. Hydrogen and oxygen maximum pressures were proportional to the initial formation rate normalized to the specific activity of the material but were not proportional to initial rate normalized to SSA. Results suggest that formation of hydrogen and oxygen is dependent on dose to the water and their consumption is dependent upon dose to them. In some materials, a back reaction forming hydrogen was observed, which may also be dependent on dose to the consumption product. $G(H_2)$-values were found to be independent of the number of MLs of adsorbed water, over the limited range studied.

INTRODUCTION

Flammable mixtures of hydrogen and oxygen within confined volumes have been a concern for a long time for handlers of plutonium dioxide material. Plutonium dioxide picks up water from humid atmospheres and reaction of the water with the material produces hydrogen.[1] If oxygen is present, a flammable mixture is possible. In some cases, both hydrogen and oxygen are produced and a flammable mixture is possible even if the confined volume was purged with an inert gas initially.[2]

This concern continues today. The most recent DOE guidance for reviewing safety analysis reports for transportation packages (SARPs) requires consideration of radiolytic decomposition of materials and that hydrogen and other flammable gases be less than 5% by volume within any confined volume.[3] The latest SARP for the 9975 requires all oxides to be dry or, if stabilized according to DOE-STD-3013 (3013 Standard), have less than 0.5 wt% moisture.[4]

A common approach to determining the hydrogen and oxygen content within a sealed container with high-purity plutonium dioxide is to assume all of the water associated with the material forms hydrogen gas and that oxygen is taken up by the material (we define a high-purity plutonium dioxide as containing more than 85% of plutonium plus americium). This approach was adopted by the 3013 Standard up to 2018. The earliest version (1994) assumed oxygen was also formed stiochiometrically, but this assumption was dropped (1996). Time can

also be used to avoid a flammable mixture by shipping quickly if the rate of hydrogen production can be reasonably estimated.[4]

Studies of the formation of hydrogen from adsorbed water on plutonium dioxide since 2000 in Russia, the US, Britain, and France have shown that (1) the rate of radiolytic hydrogen production from alpha particles is less than that of liquid water and (2) a consumption reaction limits the hydrogen pressure to well below the pressure that would result from complete radiolysis of water to hydrogen.[2, 5] These studies have identified many important parameters that affect the hydrogen pressure such as the material's specific surface area (SSA), the relative humidity (RH), the material's specific activity (SA), and the amount of water. These parameters are interrelated, for instance the SSA and RH influence the amount of water the material adsorbs. The relationships between these parameters are complex and studies that vary all parameters are required to untangle the different effects. In response to these recent studies, the 3013 Standard has adopted an approach that reduces the hydrogen pressure applying a factor to the total moisture of 0.13 to 0.25. These factors are based on empirical observations during destructive evaluations of 3013 containers as well as the recent studies demonstrating the ubiquity of back reactions.[6]

In this paper, we report on observations of hydrogen and oxygen generation in sealed containers over a broad range of SA, SSA, and RH. The question of whether the production of hydrogen is mainly radiolytic (Sims, Vladimirova, Veirs, Duffey)[2, 5a, 7] or governed by surface chemistry (Haschke)[1c] is addressed using materials with different SAs and SSAs. The maximum hydrogen and oxygen pressures within our sealed containers is addressed empirically.

EXPERIMENTAL

High-purity plutonium dioxide samples with known SSA and moisture content are placed in our small-scale reactors (~ 1/400th of a 3013 container) and the gas pressure and composition are monitored over time. The design of the small-scale reactor (SSR) system, with a total internal volume of 6.145 cm^3 has been described previously.[8] The gas sampling volume located between two sampling valves, 0.05 cm^3 (< 1 % of the SSR volume), allows the gas composition to be determined with minimal effect on the internal gas pressure. A disassembled SSR is shown in Figure 1.

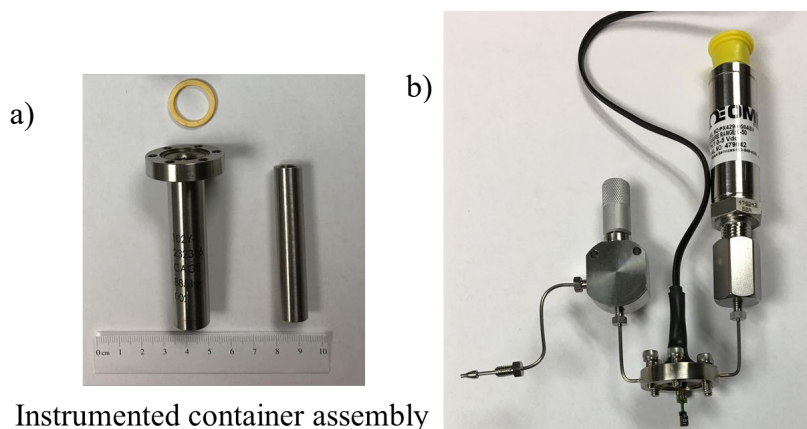
a)

b)

Instrumented container assembly

Figure 1. Disassembled SSR: a) Conflat container body with copper gasket and inner bucket and b) container lid with pressure transducer, Sensirion SHT75 RH sensor, tubing and sampling valve.

The SSRs are attached to a gas manifold for periodic sampling and analysis with an Agilent 7890 gas chromatograph (GC) calibrated for He, H_2, N_2, O_2, CO_2, CO, CH_4, NO and N_2O. Pressure, temperature, and relative humidity (RH) are monitored continuously throughout the experiment.

Material

Materials included two weapons-grade oxides produced by low-temperature calcination of plutonium (III) oxalate from Los Alamos National Laboratory (LANL) aqueous nitrate operation (PEOF and MISSTD),[9] and a reactor-grade plutonium oxide produced in the Hanford continuous oxalate precipitation and calcination process from purified nitrate solution that contains 7% Americium(BLO). Material characteristics are summarized in

Table 1. These material characteristics were determined when the material was produced initially which was many years before the studies described here were started.

Table 1. Material Physical Characteristics

	PEOF	MISSTD-1	BLO
Calcination Temperature (K)	950 °C	500-600 °C	400 °C
Specific Surface Area (SSA) 5-point (m^2 g^{-1})	1.1	21.5	5
Specific Power (mW/g)	2.1	2.1	14.2
% Actinide (Pu+Am)	87.5	85.7 (ave)	85.2
Pycnometer Density (g cm^{-3})	11.5	11.5	10.8
^{240}Pu/Pu %	6	6	18
% Am	0.1	0.2	7

Material Handling

The high-purity plutonium oxides described in Table 1 were heated in a helium atmosphere to either 400 °C, 650 °C or 950 °C to remove water and adsorbed gases such as CO_2 and NO_x. Heating plutonium oxide above the original calcination temperature reduces the SSA. The heating temperature for BLO, PEOF and MISSTD was kept low (400°C or 650°C) to minimize reduction of the SSA due to this second calcination. However, the low temperatures used for these second calcinations may not have removed all the chemisorbed water/hydroxyls and adsorbed gases. The BLO-C material BLO that was heated to a high temperature (950 °C) to reduce the SSA as well as remove adsorbed gases.

The oxides were equilibrated with water vapor above saturated solutions for approximately one week in sealed glass containers. The amount of adsorbed moisture was calculated from the weight gain. The samples with adsorbed water were transferred into the SSRs. Some moisture loss occured during transfer from the humidified chamber into the SSR in the very dry He glove box atmosphere (relative humidity < 0.1 %). Transfer time was kept to approximately 10 seconds and weight loss during transfer was assumed to be negligible. The materials with equilibrated RH indicated and their characteristics as they were loaded into the SSRs are given in Table 2.

Table 2. The materials, SSRs, SSA, SA, time between the second calcination and loading into the SSR (Δt), the second calcination temperature, sample mass, the RH the sample was equilibrated with, the amount of moisture that was adsorbed, and the calculated number of monolayers (ML) of moisture adsorbed onto the sample.

Material	SSA (m^2/g)	SA (mW g-1)	Δt (days)	T (°C)	Mass (g)	RH (%)	Moisture (wt%)	ML
BLO-33	5	14.2	11	400	7.64	33	0.39	3.5
BLO-53	5	14.2	11	400	7.67	53	0.6	5.4
BLO-53	5	14.2	7	400	7.71	53	0.59	5.4
BLO-C-33	0.8	14.2	12	950	7.02	33	0.06	3.3
BLO-C-53	0.8	14.2	19	950	7.03	53	0.07	4.2
BLO-C-75	0.8	14.2	19	950	7.01	75	0.10	5.9
MISSTD-33	20	2.1	10	400	4.83	33	1.05	2.4
MISSTD-43	20	2.1	10	400	4.83	43	1.19	2.7
MISSTD-53	20	2.1	10	400	4.83	53	1.33	3.0
MISSTD-75	20	2.1	10	400	4.83	75	1.82	4.1
MISSTD-75	20	2.1	10	400	4.76	75	1.82	4.1
PEOF-33	1.1	2.1	1435	650	8.68	33	0.046	1.9
PEOF-33	1.1	2.1	7	400	7.13	33	0.046	1.9
PEOF-58	1.1	2.1	7	400	7.14	58	0.054	2.2
PEOF-75	1.1	2.1	1435	650	9.37	75	0.069	2.9

RESULTS

In the RESULTS section, we present some of the results that best illustrate how the SA, SSA, and amount of water influence hydrogen and oxygen gas generation within sealed containers.

Gas Generation

The total pressure as a function of time, as well as the partial pressure of He, H_2, O_2, N_2, CO_2, CO, CH_4, NO and N_2O gases were recorded for all reactors. Results for BLO equilibrated at 53% RH is shown in Figure 2a. The amounts of CO_2, CO, CH_4, NO and N_2O are typically below detectable for high-purity plutonium dioxide materials. The total pressure increases initially and then decreases at a slower rate. The decrease in the total pressure is due to decreasing hydrogen and, if present, oxygen. A comparison of the hydrogen partial pressures for materials equilibrated at 75% RH is shown in Figure 2b. The time at which the hydrogen partial pressure reaches its maximum value is shorter for the higher SA material. The highest hydrogen partial pressures occur in the materials with the higher SSA. The higher SSA material has more water adsorbed than the lower SSA material.
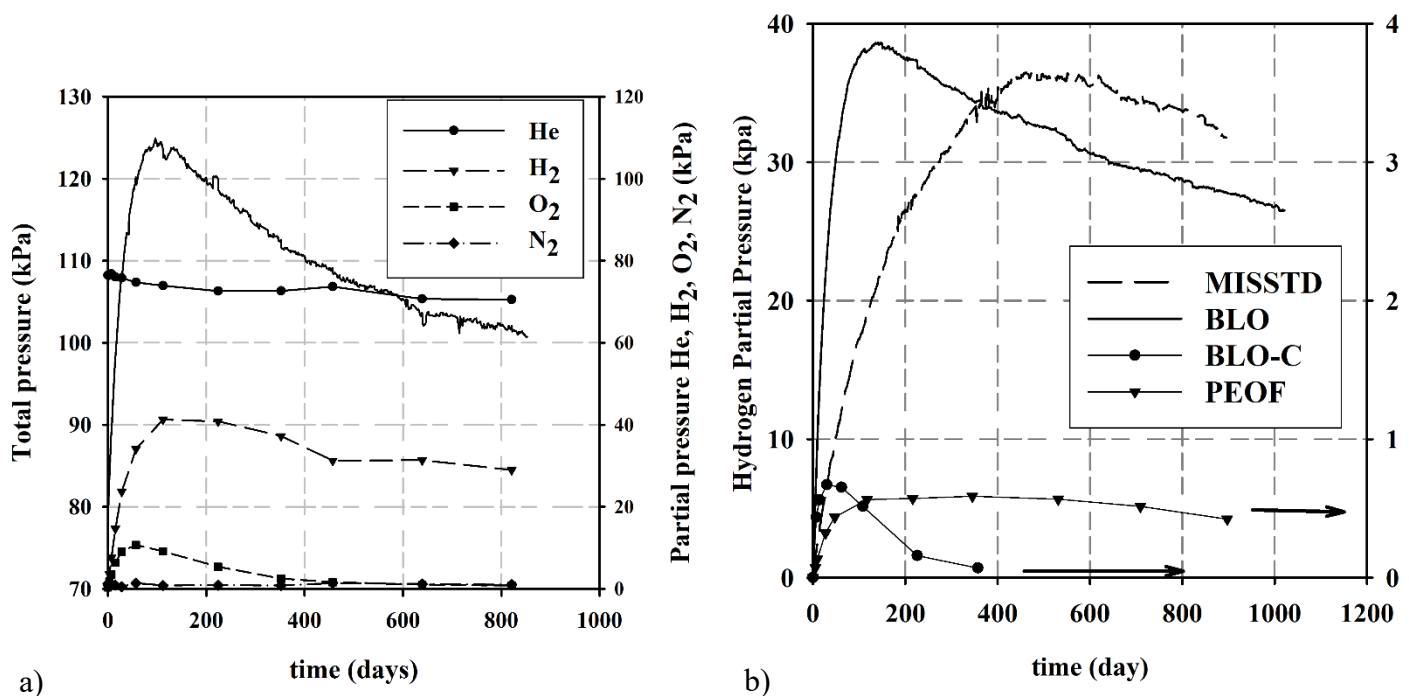

Figure 2. Gas generation. a) total pressure (left scale, solid line) and partial pressure of gases measured using a gas chromatograph as a function of time for BLO material equilibrated with 53% RH and b) hydrogen gas generation for the four materials equilibrated with 53% RH (PEOF 58%).

The hydrogen partial pressure for a particular material increases as the amount of water increases. The amount of water for a particular material increases as the RH increases. The time to reach the maximum hydrogen partial pressure generally increases with the amount water adsorbed on the material. Fitting the data to a kinetic model allows us to calculate the time to reach the maximum partial pressure and the maximum partial pressure. This was done for all of the materials and RH exposures and is shown in the fitting section.

The oxygen gas generation is similar to the hydrogen gas generation in that the materials with higher SSA (and higher water content) generate more oxygen gas. One important difference is that materials do not generate any observable oxygen gas if the hydrogen gas generation rate is low but well above detection limits. When oxygen is generated, the time to time to reach the maximum oxygen partial pressure is longer for the lower SA material, the same trend as seen in hydrogen.

<u>Flammable Gas Mixtures</u>

The amount of hydrogen and oxygen in many of the SSRs reached levels generally considered flammable. Taking 5 vol% as potentially flammable for both hydrogen and oxygen, the time to reach 5 vol% for all of the SSRs are given in Table 3. The low SSA materials BLO-C and PEOF did not generate observable oxygen. The oxygen partial pressure reached 5 vol% and then declined to below 5 vol% in the BLO-53 and BLO-53[†] reactors containing high SA and relatively high SSA material. The MISSTD material reached 5 vol% between 14 and 56 days and has not declined to less than 5 vol% after 849 days, although both gases appear to be starting to decline. The hydrogen reached 5 vol% before the oxygen for the material BLO which is high SA. The oxygen reached 5 vol% before the hydrogen for the material MISSTD which is low SA.

Table 3. The time to reach 5 vol% for hydrogen and oxygen and, for those SSRs where 5 vol% was reached, the time for the partial pressure to decline to less than 5 vol %. If the partial pressure did not decline to less than 5 vol%, the time is indicated as greater than the time of the duration of the data collection so far.

Material	Moisture wt%	Hydrogen		Oxygen	
		Days to 5%	Days to <5%	Days to 5%	Days to <5%
BLO-33	0.39	8	>1009	N/A	N/A
BLO-53	0.6	8	>1009	14	150
BLO-53	0.59	7	>821	15	112
BLO-C-33	0.06	N/A	N/A	N/A	N/A
BLO-C-53	0.07	N/A	N/A	N/A	N/A
BLO-C-75	0.10	108	108	N/A	N/A
MISSTD-33	1.05	56	>849	56	>849
MISSTD-43	1.19	56	>849	28	>849
MISSTD-53	1.33	28	>849	28	>849
MISSTD-75	1.82	14	>849	8	>849
MISSTD-75	1.82	14	>849	8	>849
PEOF-33	0.046	N/A	N/A	N/A	N/A
PEOF-33	0.046	N/A	N/A	N/A	N/A
PEOF-58	0.054	N/A	N/A	N/A	N/A
PEOF-75	0.069	324	>974	N/A	N/A

MODELING

The behavior of the hydrogen and oxygen partial pressures with time fall into two classes. In the first class, the partial pressure increases, reaches a maximum and declines back to essentially zero. The hydrogen partial pressure curve of BLO-C, Figure 3b falls into this class. All of the MISSTD curves also fall into this class at this point although the partial pressure has not declined to zero. This is modeled as first order formation and consumption by

$$H_2O \xrightarrow{k_1} H_2 \xrightarrow{k_2} sink(solid) \qquad \text{Equation 1.}$$
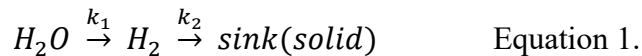
The change in H_2 pressure due to the reactions in Equation 1 is written in differential form as

$$\frac{dP_{H2}}{dt} = k_1 A(t) - k_2 P_{H2} \qquad \text{Equation 2.}$$

P_{H2} is the partial pressure of hydrogen, A(t) is the active water in the reactor involved in hydrogen generation, expressed in units of pressure using the ideal gas law, t is time in days, and k_1 and k_2 are the first-order rate constants for the formation and consumption of hydrogen in days[-1]. The model assumes exponential decay of the active water, $A(t)$, with time as shown in Equation 3, where A_0 is the amount of active water at time $t = 0$.

$$A_{H_2O}(t) = A_0 e^{-k_1 t} \qquad \text{Equation 3.}$$

The hydrogen pressure, obtained by integrating Equation 2, assuming $P_{H_2}(t)$ is $= 0$ at time $= 0$ is

$$P_{H_2}(t) = \frac{A_0 k_1}{k_2 - k_1}(e^{-k_1 t} - e^{-k_2 t}) \qquad \text{Equation 4.}$$

The initial rate is given by

$$Initial\ rate = A_0 k_1 \qquad \text{Equation 5,}$$
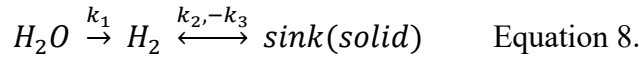
the time of the maximum pressure is given by

$$t_{max} = \frac{\ln(k_2) - \ln(k_1)}{k_2 - k_1} = \frac{\ln\left(\frac{k_2}{k_1}\right)}{k_2 - k_1} \text{Equation 6,}$$

and the maximum pressure is given by

$$P_{H_2 max} = A_0 \left[\frac{k_1}{k_2}\right]^{k_2/k_2 - k_1} \qquad \text{Equation 7.}$$

A fit to this model is shown for MISSTD hydrogen partial pressure in Figure 3a.

In the second class, the partial pressure increases, reaches a maximum and then declines to a non-zero value. The BLO material falls into this class, Figure 3b. This behavior suggests that H_2 is formed as in the first case and is consumed to form a third species that can re-form H_2. This case is modeled as first order formation with equilibrium

b)

$$H_2O \xrightarrow{k_1} H_2 \underset{}{\overset{k_2, -k_3}{\longleftrightarrow}} sink(solid) \qquad \text{Equation 8.}$$

The expression for the hydrogen pressure is

$$P_{H_2}(t) = A_0 \left(1 - e^{-k_1 t} - \frac{k_2}{k_2 + k_3}\left(1 + \frac{k_1}{k_2 + k_3 - k_1}e^{-(k_2 + k_3)t} - \frac{k_2 + k_3}{k_2 + k_3 - k_1}e^{-k_1 t}\right)\right) \qquad \text{Equation 9.}$$

The initial rate is the same as Equation 5. The time of the maximum pressure is given by

$$t_{max} = \frac{\ln\left(\frac{k_2}{k_1 - k_3}\right)}{k_2 + k_3 - k_1} \qquad \text{Equation 10.}$$

The maximum pressure is given by a complicated expression too long to show. The H_2 pressure at long times is given by

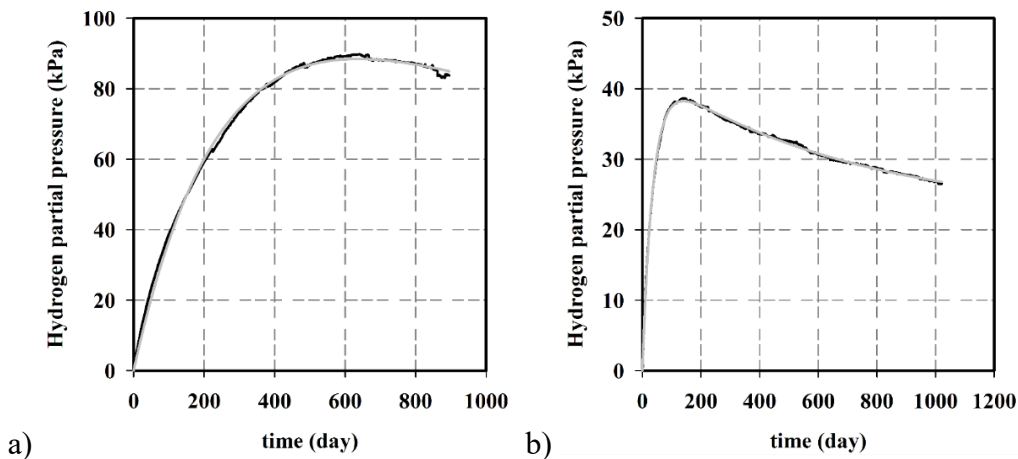$$P_{H_2}(t \to \infty) = A_0 \frac{k_3}{k_2 + k_3} \qquad \text{Equation 11.}$$

Figure 3. a) the hydrogen partial pressure data (black) and the fit to Equation 4 (gray) for MISSTD equilibrated to 75% RH. b) Fit to Equation 9 for BLO material equilibrated to 75% RH.

The same equations hold true for the generation of oxygen; substitute oxygen for hydrogen. There are many chemical reactions that occur when water adsorbs radiation energy to produce hydrogen or oxygen. These complex chemical reactions overall behavior seems to be captured by these simple rate equation.

Values of the fitting parameters obtained from fitting Equation 4 or Equation 9 to the hydrogen and oxygen pressure data versus time with a non-zero intercept to allow for some air in the reactor are shown in Table 4. Values for the initial rate and maximum pressure are derived from the data with far less uncertainty than the values for the rate constants. The ratio of the maximum pressure of hydrogen observed (P_{max}) to the moles of water added to the material when expressed in units of pressure ($P_{initial}$) represents the fraction of the available water pressurizing the container. This is given in Table 4 as $P_{max}/ P_{initial}$ and ranges from 0.3 to 4.3. This range is consistent with results seen during destructive evaluation of 3013 containers. This appears to be the result of (1) only a fraction of the water participates in radiolysis and (2) a hydrogen consumption reaction that removes hydrogen gas.

Table 4. The results from fitting the hydrogen and oxygen pressure data. Equation 4 was used for BLO-C and MISSTD. Equation 9 was used for BLO and PEOF. The initial rate, maximum pressure, and time to maximum pressure are derived from the fitting parameters.

Material	K_1 (day^{-1})		K_2 (day^{-1})		K_3 (day^{-1})		Initial Rate (kPa day^{-1})		P_{max} (kPa)		t_{max} (day)		$\frac{P_{max}}{P_{initial}}$ (%)
	H_2	O_2	H_2	O_2	H_2	O_2	H_2	O_2	H_2	O_2	H_2	O_2	H_2
BLO-33	3.8E-3	6.3E-3	2.2E-2	2.7E-2	1.7E-3	0	0.46	0.05	16	1	120	70	2.1
BLO-53	1.5E-3	9.4E-3	2.7E-2	2.5E-2	7.6E-4	2E-4	1.15	0.39	38	9	140	63	3.2
BLO-53	2.6E-3	6.0E-3	2.1E-2	3.7E-2	1.3E-3	1E-4	1.11	0.55	42	11	143	59	3.5
BLO-C-33	6.7E-3	----	1.8E-1	----	----	----	0.07	----	0.4	----	19	----	0.3
BLO-C-53	7.1E-3	----	8.2E-2	----	----	----	0.07	----	0.7	----	33	----	0.5
BLO-C-75	3.2E-3	----	2.0E-2	----	----	----	0.13	----	4	----	110	----	2.4
MISSTD-33	3.3E-4	2.8E-3	5.3E-3	2.8E-3	----	1E-3	0.14	0.09	21	13	556	436	1.7
MISSTD-43	2.3E-4	3.7E-3	6.2E-3	3.7E-3	----	2E-3	0.18	0.19	25	22	552	403	1.8
MISSTD-53	6.2E-4	3.9E-3	4.2E-3	3.9E-3	----	2E-3	0.21	0.26	36	28	532	390	2.3
MISSTD-75	4.2E-4	4.9E-3	3.9E-3	5.0E-3	----	5E-3	0.45	0.61	88	61	636	759	4.1
MISSTD-75	6.3E-4	4.6E-3	3.1E-3	7.5E-3	----	5E-3	0.42	0.70	90	64	639	849	4.3
PEOF-33	4.2E-3	----	1.9E-2	----	5.5E-4	----	0.01	----	0.2	----	107	----	0.4
PEOF-33	8.2E-4	----	2.6E-2	----	0	----	0.01	----	0.4	----	139	----	0.5
PEOF-58	3.7E-4	----	2.5E-2	----	0	----	0.02	----	0.6	----	170	----	0.6
PEOF-75	1.1E-3	----	7.3E-3	----	2.0E-3	----	0.03	----	3.9	----	491	----	2.3

RADIOLYSIS OR CHEMICAL (SURFACE) REACTIONS

Higher specific activity materials have higher initial rates of hydrogen generation for material with similar amounts of water suggests that the formation reaction is dependent on radiolysis. In addition, higher specific activity materials result in shorter time to maximum pressures for the same initial rate. This suggests a higher rate of consumption in materials with higher specific activity. Normalizing the initial hydrogen and oxygen generation rates to the SA of the material places the data for each species on a single line as shown in Figure 4. The hydrogen P_{max} has a slope of 400 day(W/kg) when plotted with respect to the initial rate of hydrogen generation normalized to the SA. The oxygen P_{max} has a slope of 200 day(W/kg).

This dependence of P_{max} upon the specific activity suggests that the formation and consumption of hydrogen and oxygen is due to radiolysis. Since k_1, k_2, and where applicable, k_3 all contribute to P_{max}, a constant slope is only possible if all three rate constants are proportional to specific power by the same amount. This trend was not observed when normalizing to specific surface area.

These results suggest that it may be possible to predict the maximum hydrogen partial pressure in a closed system containing high purity oxide knowing only the SA and the initial rate of hydrogen and oxygen

generation. The initial rates can be estimated using the amount of water, the SA, and the G-values (number of molecules produced per 100 eV of adsorbed dose).
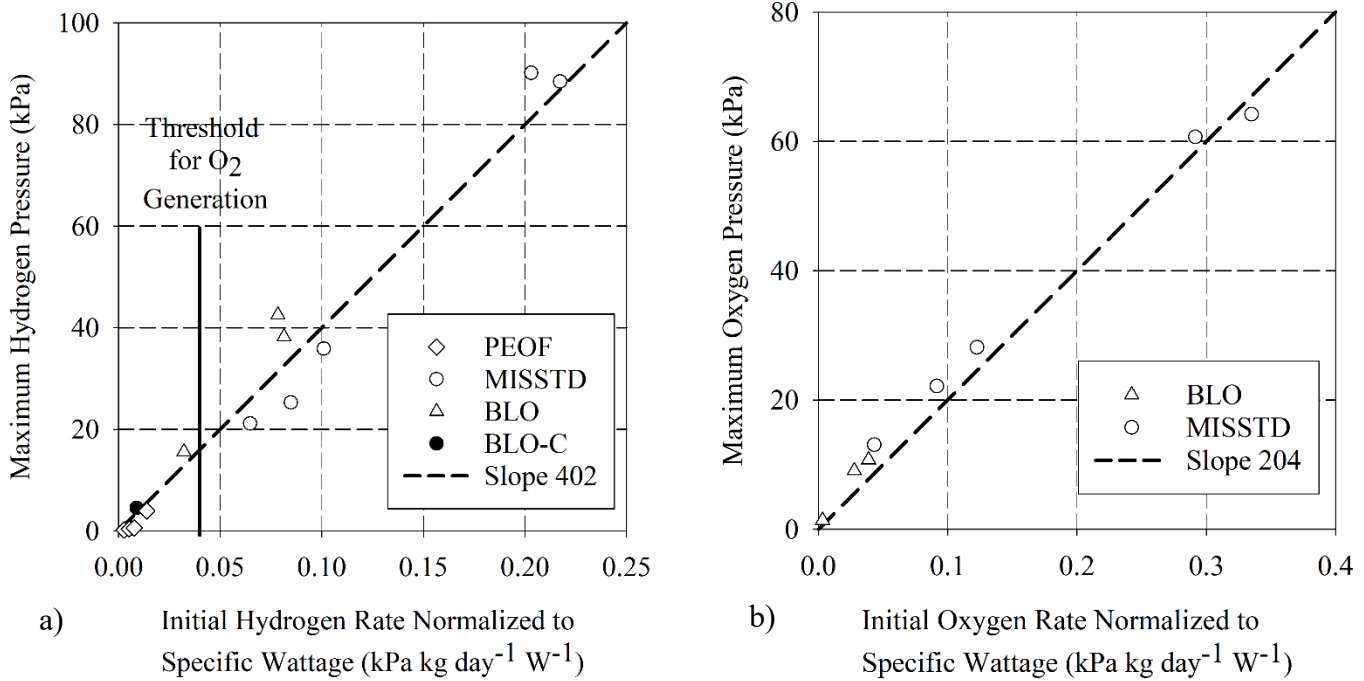

a) Initial Hydrogen Rate Normalized to Specific Wattage (kPa kg day^{-1} W^{-1})

b) Initial Oxygen Rate Normalized to Specific Wattage (kPa kg day^{-1} W^{-1})

Figure 4. The maximum pressures for a) hydrogen and b) oxygen versus the initial gas generation rate normalized to the material SA.

DETERMINATION OF G-VALUES

Determination of G-values is a common method for expressing the radiolytic generation of chemical species in a system. G-values are defined as the number of molecules produced per 100 eV of adsorbed dose. An expression for an initial $G(H_2)$ using the fitting parameters and the material properties is:

$$G_{value} = \frac{initial\ rate}{dose} = \frac{A_0 k_1}{SA * m_{H_2O} \frac{S_{H_2O}}{S_{mat}}} = k_1 A_0 \frac{V_g N_A}{R\,T} \frac{day}{86400\ s} \frac{1}{SA \frac{6.2418 \times 10^{18}\ eV/100}{s\ W} m_{H_2O}} \frac{1}{\frac{S_{H_2O}}{S_{mat}}} \qquad \text{Equation 12}$$

Table 5. Summary of the number of ML and the G-values for hydrogen and oxygen.

Material	ML	G(H$_2$)	G(O$_2$)	G(H$_2$)/ G(O$_2$)
BLO-33	3.5	0.07	0.08	0.9
BLO-53	5.4	0.12	0.04	3.0
BLO-53	5.4	0.11	0.06	1.8
BLO-C-33	3.3	0.08	----	----
BLO-C-53	4.2	0.07	----	----
BLO-C-75	5.9	0.08	----	----
MISSTD-33	2.4	0.09	0.06	1.5
MISSTD-43	2.7	0.10	0.11	0.9
MISSTD-53	3.0	0.11	0.13	0.8
MISSTD-75	4.1	0.17	0.23	0.7
MISSTD-75	4.1	0.16	0.27	0.6
PEOF-33	1.5	0.06	----	----
PEOF-33	1.9	0.10	----	----
PEOF-58	2.2	0.13	----	----
PEOF-75	2.9	0.14	----	----

m_{H2O} is the mass of water associated with the material (g), R is the ideal gas constant in the appropriate units, T is the temperature in degrees K, V_g is the free gas volume, N_A is Avogadro's number, SA is the material specificactivity (W g^{-1}), S_{H2O}/S_{mat} is the ratio of the stopping power of alpha radiation in water to that of plutonium dioxide and is essentially constant at 3.6 for high-purity plutonium dioxide. For this study *m_{H2O} was taken to be the amount of water adsorbed on the samples during equilibration*. A smaller value, such as A_0 determined from the fit, could be used which would result in a significantly higher G-value. Table 5 summarizes the monolayers of water and G-values for each reactor. The ratio of G(H$_2$)/ G(O$_2$) varies significantly from the expected value of two for the decomposition of water.

Our data suggest G(H$_2$) for high purity oxides is approximately constant at 0.1 molecules 100 eV^{-1}, independent of the number of monolayers over the limited range covered in this study. Results published by Sims et.al over a larger range of ML of water suggested that G(H2) increases with increasing number of ML of water.[5a] Figure 5 compares the results from this study with those reported by Sims.
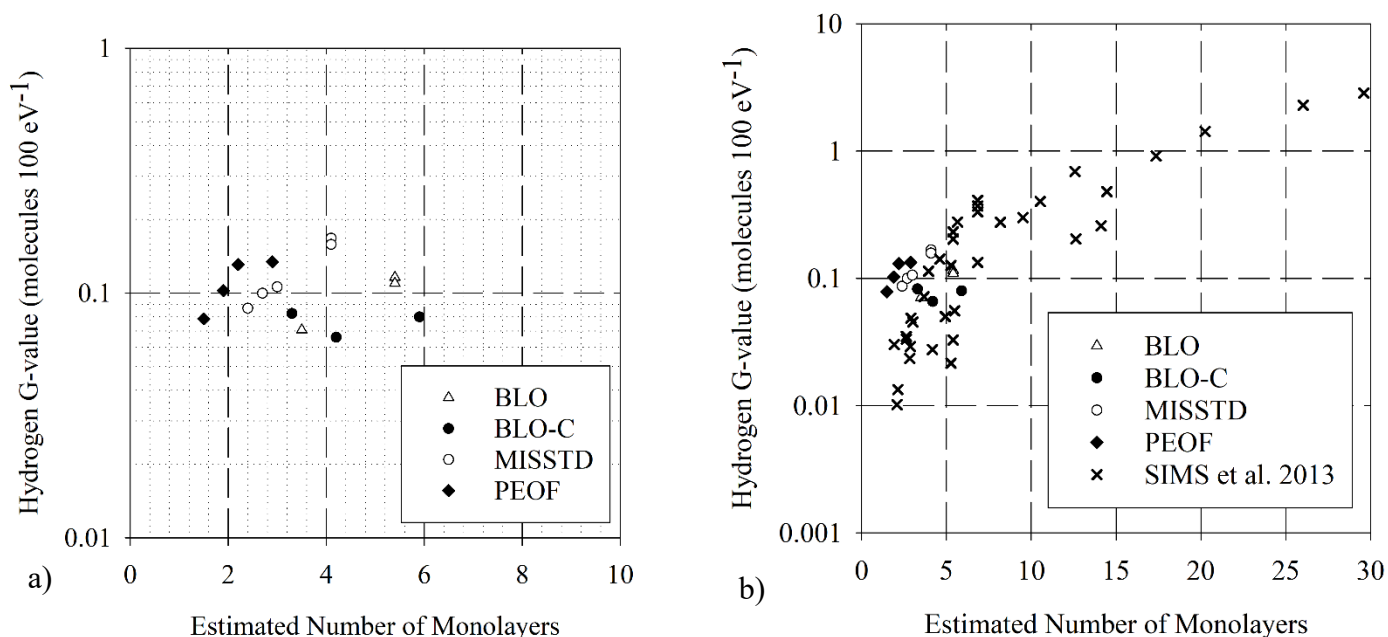

Figure 5. Hydrogen G-values versus number of monolayers a) from this study and b) compared to Sims et al.

CONCLUSION

The observed pressurization within sealed containers is much lower than expected assuming all of the water undergoes radiolysis to form H$_2$ gas. The maximum hydrogen pressure was a small fraction (0.3 to 4.3%) of the pressure expected if all of the water associated with the material forms hydrogen gas and none of the hydrogen gas is consumed. This range is consistent with results seen during destructive evaluation of 3013 containers. This appears to be the result of (1) only a fraction of the water participates in radiolysis and (2) a hydrogen consumption reaction that removes hydrogen gas. Oxygen is also generated at the same time. Flammable mixtures occur that can persist for years. The observed hydrogen and oxygen pressures can be fit using relatively simple rate equations. The generation of hydrogen and oxygen is shown to arise from radiolysis. An empirical relation is described between the maximum hydrogen and oxygen pressures and the initial rates normalized to the specific activity of the material. G-values are consistent with literature, but the dependence on monolayers of water is not observed. There is a threshold in the rate of hydrogen generation below which oxygen is not observed. The results reported here are for a single sized sealed container. Different sealed container volumes and geometry have not been investigated and may result in different behavior.

ACKNOWLEDGEMENTS

REFERENCES

1.   (a) Stakebake, J. L.; Dringman, M. R. *Hygroscopicity of plutonium dioxide*; RFP-1056; Dow Chemical Company: Golden, CO, 1968; (b) Haschke, J. M.; Ricketts, T. E., Adsorption of water on plutonium dioxide. *Journal of Alloys and Compounds* **1997,** *252*, 148-156; (c) Haschke, J. M.; Allen, T. H.; Morales, L. A., Reaction of Plutonium Dioxide with Water: Formation and Properties of PuO_{2+x}. *Science* **2000,** *287*, 285-286; (d) Benhamou, A.; Beraud, J. P., Reprise d'humidite par une poudre d'oxyde de plutonium. *Analusis* **1980,** *8*, 376-380.

2.   (a) Vladimirova, M. V.; Kulikov, I. A., Formation of H_2 and O_2 in Radiolysis of Water Sorbed on PuO_2. *Radiochemistry* **2002,** *44* (1), 86-90; (b) Veirs, D. K.; Berg, J. M.; Narlesky, J. E.; Trujillo, L.; Romero, E. L.; Wilson, J., K.V. In *Hydrogen and Oxygen G-values from Water Adsorbed onto Plutonium Dioxide*, Plutonium Futures - The Science 2014, Las Vegas, NV, Blobaum, K., Ed. American Nuclear Society: Las Vegas, NV, 2014.

3.   DiSabatino, A. A.; Biswas, D.; DeMicco, M.; Fischer, L. E.; Hafner, R. S.; Hagler, L. B.; Haslam, J. J.; Mok, G. C.; Patel, C. S.; Russell, E. W.; Sitaraman, S.; Syn, C. K.; Wen, J.; West, M. H. *Packaging Review Guide for Reviewing Safety Analysis Reports for Packagings*; UCID-21218 Rev. 3; Lawrence Livermore National Laboratory: Livermore, CA, 2008.

4.   Department of Energy *Safety Analysis Report for Packaging Model 9975*; S-SARP-G-00003, Revision 2; Savannah River Operations: Aiken, SC, 2013.

5.   (a) Sims, H. E.; Webb, K. J.; Brown, J.; Morris, D.; Taylor, R. J., Hydrogen yields from water on the surface of plutonium dioxide. *Journal of Nuclear Materials* **2013,** *437* (1-3), 359-364; (b) Venault, L.; Deroche, A.; Gaillard, J.; Lemaire, O.; Budanova, N.; Vermeulen, J.; Maurin, J.; Vigier, N.; Moisy, P., Dihydrogen H_2 steady state in α–radiolysis of water adsorbed on PuO_2 surface. *Radiation Physics and Chemistry* **2018**.

6.   Department of Energy *Stabilization, Packaging, and Storage of Plutonium-Bearing Materials*; DOE-STD-3013-2018; U.S. Department of Energy: Washington, D.C. 20585, 2018.

7.   Duffey, J. M.; Veirs, D. K.; Berg, J. M.; Livingston, R. R., Pressure Development in Sealed Containers with Plutonium-bearing Materials. *Journal of Nuclear Material Management* **2010,** *37* (3), 32-42.

8.   Veirs, D. K.; Worl, L. A.; Harradine, D. M.; Martinez, M. A.; Lillard, S.; Schwartz, D. S.; Puglisi, C. V.; Padilla, D. D.; Carrillo, A.; McInroy, R. E.; Montoya, A. R. *Gas generation and corrosion in salt-containing impure plutonium oxide materials: Initial results for ARF-102-85-223*; LA-UR-04-1788; Los Alamos National Laboratory: Los Alamos, NM, 2004.

9.   Berg, J. M.; Narlesky, J. E.; Veirs, D. K. *A summary of volatile impurity measurements and gas generation studies on MISSTD-1, a high-purity plutonium oxide produced by low-temperature calcination of plutonium oxalate*; LA-UR-12-21473; Los Alamos National Laboratory: Los Alamos, NM, 2012.